An electrochemically controlled supramolecular zip tie based on host-guest chemistry of CB[8]

ARTICLE

An electrochemically controlled supramolecular zip tie based on host-guest chemistry of CB[8]

Iago Neira,[a] Olaya Domarco,[a] Jose L. Barriada,[a] Paola Franchi,[b] Marco Lucarini,[b] Marcos D. García*[a] and Carlos Peinador*[a]

The interaction of a series molecular axles incorporating two viologens and an electron-rich aromatic unit with CB[8] was studied revealing a zip tie mechanism driven by the reduction of the viologen units.

Introduction

Supramolecular switches are defined as host-guest assemblies, composed of two or more interacting units, whose association can be transiently controlled by the external stimulation, such as light, electrical potential, or chemical effectors.[1] The interest in such systems is manifold,[2] as they can be used in man-controlled practical applications such as the development of stimuli–responsive catalysis,[3] materials[4] or molecular machines.[5] In this scenario, the host-guest chemistry of cucurbit[n]uril (CB[n]s),[6,7] represents a versatile platform for the development of the above-mentioned stimuli-responsive architectures, especially relevant on the case of CB[8], due to its ability to form stimuli-responsive 1:2 homo and heteroternary complexes with appropriate guests.[8] In this context, viologens (N,N'-dialkyl-4,4'-bipyridinium derivatives),[9,10] have been extensively used in conjunction with CB[8], as these π-acceptors are able to form different redox-responsive complexes (i.e. 1:1 or 1:2 homoternary aggregates depending on the reduction state of the salt, and 1:2 heteroternary complexes with appropriate aromatic π-donors as second guests). In both cases, the appropriate reversibility of the redox processes, allows for an easy swapping between the 1:1 homoternary complex, formed radical pairing of two reduced viologens, and the non-stimulated form of the responsive aggregate.

Continuing our interest on the use of pyridinium salts as building blocks in supramolecular chemistry,[11] and the development of new CB[n]-based host:guest chemistry,[12] we present herein the design and study of the supramolecular translocation switches $\mathbf{1}$-$\mathbf{3} \subset CB[8] \rightleftarrows \mathbf{1'}$-$\mathbf{3'} \subset CB[8]$, envisioned to produce the controlled gliding of the macrocyclic subunit of the

pseudorotaxane by appropriate redox stimulation. The threads $\mathbf{1}$-$\mathbf{3}$ are composed by two 4,4'-bipyridinium units (terminal $bipy_t^{2+}$ and internal $bipy_i^{2+}$), connected by an oligo ethylene chain of variable length, and a 2-hydroxynaphthalene unit attached to $bipy_i^{2+}$ by a rigid p-xylene linker (Scheme 1). This connection was designed to prevent the simultaneous complexation of $bipy_i^{2+}$ and naphthalene units inside CB[8], and to ensure the maintenance of the loop during the operation of the zip tie.[13] In its non-stimulated state, the $bipy_t^{2+}$ and naphthalene (NAP) units are located inside CB[8] in an end-to-end pseudorotaxane with no loop formation. Upon reduction, the supramolecular switch changes to an end-to-interior state, with a viologen cation radical dimer formed inside the cavity and the concomitant appearance of the loop. Although similar end-to-end/end-to-interior systems have been reported by Kim and Stoddart (Scheme 1),[14] our switch potentially allows a strict control over loop formation extension and contraction, paving the way for their prospective use on the controlled catch and release of cations by the oligo ethylene-containing loop.
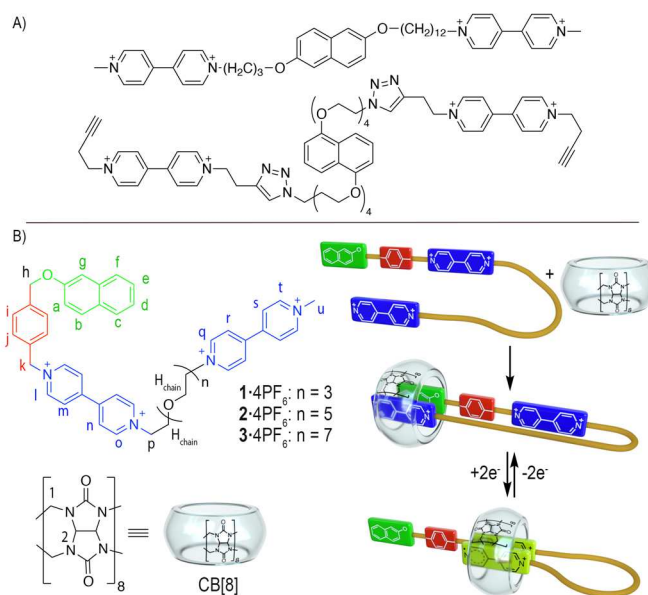
Scheme 1: A) Structures of axles reported by Kim (top) and Stoddart (bottom). B) Structures of axles $\mathbf{1^{4+}}$-$\mathbf{3^{4+}}$ described in this work, CB[8] and schematic

a. Departamento de Química and Centro de Investigaciones, Científicas Avanzadas (CICA), Universidade da Coruña, Facultad de Ciencias, E-15071 A Coruña, Spain. E-mail: carlos.peinador@udc.es, marcos.garcia1@udc.es.
b. Department of Chemistry "G. Ciamician" – Alma Mater Studiorum-University of Bologna, Via San Giacomo 11, Bologna, Italy.
† Electronic Supplementary Information (ESI) available: Synthetic procedures, characterization data for all new compounds and host-guest complexes See DOI: 10.1039/x0xx00000x

representation of the expected complexation modes for the supramolecular zip tie studied in this work.

Results and discussion

Synthesis and characterization of molecular components

Regarding the thread components of the zip ties, molecules 1^{4+}-3^{4+} were synthesized from commercially-available 2-naphthol, 4,4'-bipyridine, 1,4-dibromomethyl benzene and the corresponding oligo(ethylene glycol) dibromides, by using a series of nucleophilic substitutions (see Supporting Information). Compounds 1^{4+}-3^{4+} were adequately characterized by standard spectroscopic techniques, including ^{1}H NMR and ^{13}C NMR spectroscopy, as well as high-resolution mass spectrometry.
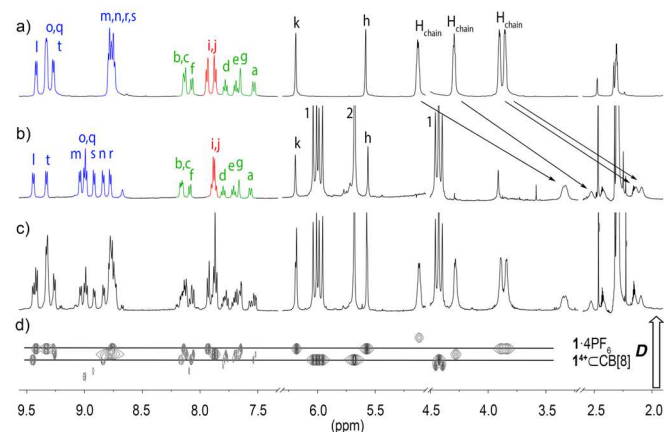

Figure 1. Partial ^{1}H NMR (D$_2$O/CD$_3$CN 3:2, 500 MHz) spectrum of: a) **1** 4PF$_6$ (2 mM); b) equimolar solution of **1** 4PF$_6$ (2 mM) and CB[8]; c) a solution of **1** 4PF$_6$ (2 mM) and CB[8] (1 mM); d) DOSY NMR experiment of solution c). Proton numbering is given in Scheme 1.

Interaction between axles 1^{4+}-3^{4+} and CB[8]

Addition of an excess of CB[8] to a 2 mM solution of thread $1\cdot$4PF$_6$ in D$_2$O/CD$_3$CN (3:2, v/v), leads to the formation of a 1:1 adduct ($1^{4+}\subset$CB[8]), as corroborated by ESI-MS showing the losses of one and two PF$_6$ anions at, respectively, m/z = 1176 and 736. The ^{1}H NMR of this species shows as well symptomatic resonances in good agreement with the complexation taking place. For instance, while the signals corresponding to the naphthol or phenylene moieties remain unchanged, some of the resonances for the methylene groups in the oligo ethylene chain are significantly shifted upfield, as well as those protons of the viologen moieties shifted to higher frequencies (Figure 1). On the other hand, the observed splitting for the signals of the CB[8] protons, points out to a different chemical environment in both portals. Further evidence of the nature of the aggregate was derived from the ^{1}H NMR spectrum of a 1:0.5 mixture of 1^{4+}:CB[8] at r.t., which displays signals resulting from the slow kinetic exchange on the ^{1}H NMR timescale between complexed and uncomplexed states. Finally, the kinetic entanglement of the CB[8] and $1\cdot$4PF$_6$ components of the pseudorotaxane is apparent from DOSY experiments, which show that the proton resonances arise for the new species correlates with a larger

hydrodynamic radii than that of the individual components (Figure 1d). Taking into account all these observations, it can be assumed the formation of a [2]pseudorotaxane where the oligo methylene chain is located inside the CB[8] cavity, with the positive charges of the bipyridinium ring interacting with the carbonyl groups of CB[8]. The observed preference of this binding mode over the formation of the intramolecular heteroternary charge transfer complex involving the bipy$_t$$^{2+}$ and NAP moieties is not surprising, accounting for the inadequate extension of the olygo ethylene linker on $1\cdot$4PF$_6$.

UV-visible spectroscopy was employed to monitor the interaction between $1\cdot$4PF$_6$ and CB[8] in H$_2$O/CH$_3$CN (3:2, v/v). The decrease in the peak at 261 nm concomitant to the increase in the concentration of CB[8], fits to a 1:1 binding model with a K_a = (1.97 ± 0.2) × 10^5 L mol^{-1}. The fitting curve shows a inflection point at *ca*. $\chi_{CB[8]}$ = 0.5, and a second isotherm indicating a 1:2 stoichiometry when an excess of cucurbituril is added (see Supporting Information). This behavior has been observed before by Kaifer *et al.* in similar systems.[15] It should be noted that the 1:2 complex cannot be observed in NMR experiments, due to the low solubility of CB[8] in most solvents, which does not allow to detect a significant excess of free CB[8] by this technique.

In clear contrast with the data compiled for $1\cdot$4PF$_6$, the binding between CB[8] and $2\cdot$4PF$_6$ or $3\cdot$4PF$_6$ resulted in a ^{1}H NMR spectra showing broad signals as a result of a situation near to coalescence for the equilibrium on the technique's timescale. Conversely, the ^{1}H NMR spectra recorded at 343 K allowed the detection of defined signals, but did not showed the remarkable upfield shifts of the oligo methylene chain protons observed in $1^{4+}\subset$CB[8], ruling out the insertion of the linker inside the macrocyclic host. Moreover, the NAP protons were the resonances more affected by coalescence in this occasion, suggesting the establishment of intramolecular charge transfer complexes. The formation of the [2]pseudorotaxanes $2^{4+}\subset$CB[8] and $3^{4+}\subset$CB[8] was also supported by ESI-HRMS, which showed peaks resulting from the loss of two and three hexafluorophosphate ions, and with isotopic distributions in very good agreement to those theoretically calculated (Figure 2).
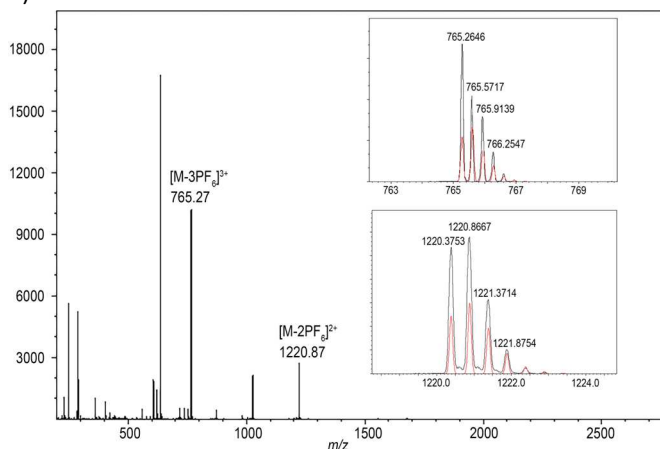

Figure 2. LR ESI-MS spectrum, for $2^{4+}\subset$CB[8] showing the loss PF$_6$ fragments. Insets: HR ESI-MS isotopic distributions for some of the most relevant peaks (experimental peaks in black, calculated peaks in red).

Finally, the interaction between threads 1^{4+}-3^{4+} and CB[8] was investigated in pure organic media. Consequently, the ^{1}H NMR spectra of 1-3·4PF$_6$⊂CB[8] in CD$_3$CN showed a similar behaviour for the three systems, with the upfield shift experienced by the protons of the oligo ethylene chains, supporting the relative location of the 2-3·4PF$_6$ threads relative to CB[8] as analysed for 1·4PF$_6$⊂CB[8] in aqueous media.

Electrochemical and UV-Vis studies of the zip tie mechanism

In order to achieve a deeper insight into the structure of the inclusion complexes obtained, both in their reduced and oxidized forms, we carried out cyclic voltammetry and UV-Vis spectroscopy studies for those systems. Therefore, the redox properties of linear components 1-3·4PF$_6$ in absence and presence of CB[8] were measured in H$_2$O/CH$_3$CN (3:2, v/v). As expected, in absence of CB[8], the threads show two voltammetric waves at *ca*. -0.48 and -0.93 V *vs* Ag/AgCl, with a sharp second peak that indicates a strong adsorption of the fully reduced species on the surface of the electrode. Each of these waves represents the uptake of two electrons, one by each of the viologen residues, which behave as essentially independent units, revealing no apparent electronic communication among them.
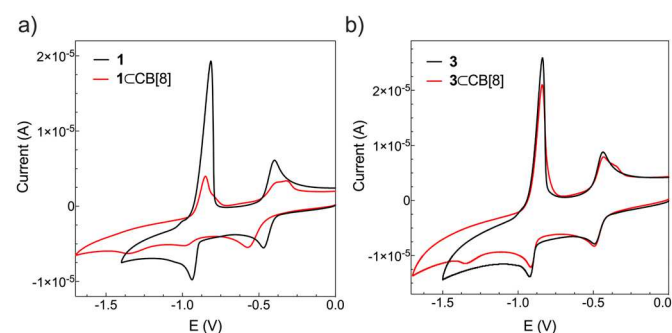

Figure 3. Superposed cyclic voltammetric response on a glassy carbon electrode of: a) 1.0 mM 1 4PF$_6$ (black line), 1.0 mM 1^{4+}⊂CB[8] (red line) and b) 1.0 mM 3 4PF$_6$ (black line), 1.0 mM 3^{4+}⊂CB[8] (red line). Supporting electrolyte: 0.1 M KCl. Scan rate: 50 mV/s.

On the other hand, the cyclic voltammogram of 1^{4+}⊂CB[8] shows significant differences with that of the free thread, with the first reduction peak remarkably shifted (ΔE = -99 mV), supporting the initial proximity of the viologen moieties to the CB[8] portals, and indicating a fast shuttling of the host between bipy$_t^{2+}$ and bipy$_i^{2+}$ (Figure 3). On the contrary, 2^{4+}⊂CB[8] and 3^{4+}⊂CB[8] presented an unaltered first reduction potential when compared with free threads. These first reduction peaks for 2^{4+}⊂CB[8] and 3^{4+}⊂CB[8] consist of two closely overlapping peaks, corresponding to two electrochemically different viologen units: one resulting from a CT complex between NAP and bipy$_t^{2+}$ inside CB[8], while the other in good agreement with the non-interacting bipy$_i^{2+}$ unit. A third reduction wave around -1.35 V corresponds to the species with the reduced units bipy$_t^{+\cdot}$ and bipy$_i^{+\cdot}$ paired inside CB[8] upon the first reduction is produced. Interestingly, the third reduction peak (also in 1^{4+}⊂CB[8]) is more visible at slower rather than faster scan rates reflecting the fact that the formation of [(bipy$_t^{+\cdot}$)(bipy$_i^{+\cdot}$)]⊂CB[8] is slow in the CV time scale (see Supporting Information). At fast scan rates (0.5 Vs^{-1}) the intermediate

reduction peak at -0.9 V associated to no interacting bipy$_i^{+\cdot}$ and bipy$_t^{+\cdot}$ is cleary more intense than the third peak indicating the residual formation of [(bipy$_t^{+\cdot}$)(bipy$_i^{+\cdot}$)]⊂CB[8].

Addition of an excess of Na$_2$S$_2$O$_4$ to solutions of 1^{4+}-3^{4+}⊂CB[8] caused an immediate change of colour to intense purple. The UV-Vis spectra of these solutions show an intense and no structured band (e.g. λ_{max} = 523 nm for 2^{4+}⊂CB[8]), characteristic of the cation radical species.[14b]

EPR measurements

Further evidence supporting the looped structures for the inclusion complexes in aqueous media when 1^{4+}-3^{4+} are reduced in the presence of CB[8], were obtained by EPR spectroscopy. Bipyridinium radical cations were generated inside the EPR cavity by *in situ* reduction in carefully deoxygenated H$_2$O/CH$_3$CN (3/2, v/v) solutions of the diamagnetic precursors 1^{4+}-3^{4+} with excess Na$_2$S$_2$O$_4$ (5–10 equiv.), both in the absence and presence of CB[8]. Reduction of 1^{4+}-3^{4+} in the absence of CB[8] resulted in strong EPR spectra which show a partially resolved complex multiline pattern centered at g = 2.0031 (see Figure 4). Although the poor resolution of hyperfine structure on the EPR did not allow us to determine the values of the corresponding hyperfine splitting constants, both g-factor and overall splitting (ca. 30 G), are in agreement with EPR parameters reported in the literature for the viologen radical cations.[16] Furthermore, The EPR spectrum is consistent with the simple superposition of the signals deriving from the two different viologen units. Since these two viologens are characterized by a different substitution pattern in one pyridine ring (a methylene unit is replaced by a methyl group in the terminal unit 1^{4+}-3^{4+}), the EPR spectra are expected to show a partial overlap of the spectral lines, with a consequent loss of spectra resolution. According to the electrochemical measurements discussed-above, we can conclude that, in the absence of CB[8], each of viologen residues behave as essentially independent units and no apparent electronic communication is observed among them. In some experiments, a second weak single line signal was also detected (see Supporting information). This impurity signal, centered at g-factor=2.0061 corresponds to the SO$_2^{•-}$ radical anion and is the result of the known equilibrium of dithionite with its two dissociated SO$_2^{•-}$ radical anions.[17]

Figure 4.
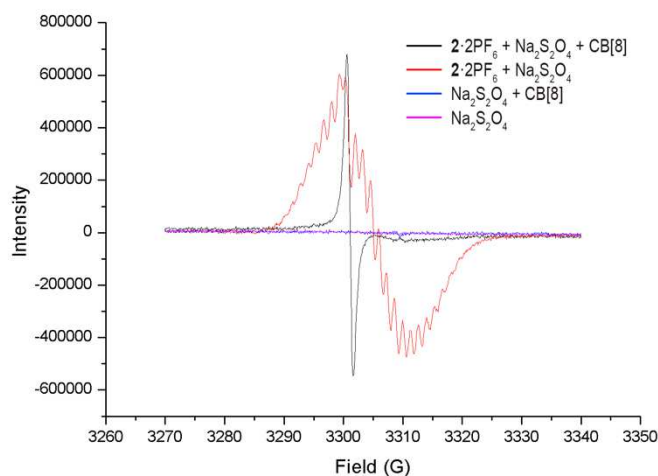
When $\mathbf{1^{4+}}$-$\mathbf{3^{4+}}$ precursors are instead reacted with $Na_2S_2O_4$ in the presence of CB[8] under the same experimental conditions, the EPR spectrum is mainly characterized by the presence of the signal due to $SO_2^{\bullet-}$ and a very weak signal due to viologen radical cation. In most cases the signal due to viologen cation is so weak that is hardly detectable (see figure 4). It is well known that viologen radical cations dimer are diamagnetic and thus, EPR silent.[18] Consequently, the absence of the viologen radical cation EPR signal observed in the presence of the macrocycle is coherent with the formation of a diamagnetic EPR-silent dimer $(bipy_t^{+\bullet})(bipy_i^{+\bullet})$ inside the cavity of CB[8] itself.

In principle, the absence of an EPR signal for viologen radical cation could also be attributed to the inhibition by CB[8] of the reductive reaction. This hypothesis, however, can be discarded because of the detection of the EPR signal due to $SO_2^{\bullet-}$ whose formation can be related to the occurrence of the reaction between $\mathbf{1^{4+}}$-$\mathbf{3^{4+}}$ and dithionite. Actually, no EPR signals were visible when $Na_2S_2O_4$ was simply dissolved in the solution or mixed with CB[8] alone (see Figure 4).
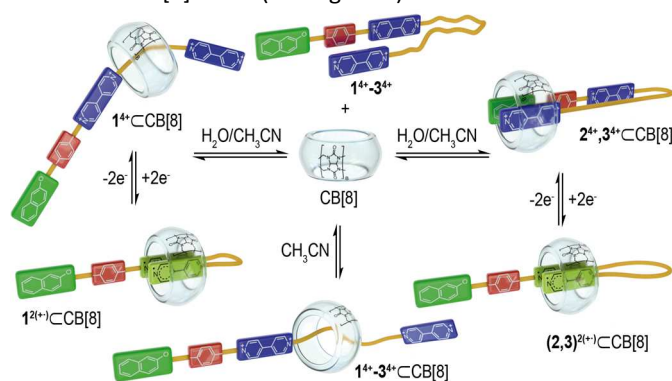

Figure 5. Cartoon representation of the different interaction modes of $\mathbf{1^{4+}}$-$\mathbf{3^{4+}}$ with CB[8] in aqueous and organic media.

Conclusions

In summary, three molecular axles composed by an aromatic electron-rich system and two viologen units connected by a oligo ethylene chain were synthesized. In aqueous media and in presence of CB[8] the longer axles $\mathbf{2^{4+}}$ and $\mathbf{3^{4+}}$ locate one of the bipyridinum units and the naphthol ring inside the CB[8] cavity. In contrast, the shorter chain of $\mathbf{1^{4+}}$ prevents this insertion mode forcing the CB[8] to move towards the oligo ethylene chain (Scheme 5). Therefore, the eleven atom chain in $\mathbf{1^{4+}}$ is not long enough to allow the simultaneous insertion in the cavity of CB[8] of naphtol and $bipy_t^{2+}$ moieties. Monoelectronic reduction of each bipyridinium unit in $\mathbf{1^{4+}}$-$\mathbf{3^{4+}}$⊂CB[8] resulted in the cation-radical species which are moved into the CB[8] inducing the axle movement and the loop formation in the oligo ethylene chain. In organic media the three axles showed the same behaviour with the oligo ethylene chain inside the CB[8]. Undoubtedly, the absence of hydrophobic interactions and entropic factors favours the formation of these complexes. Further investigation into cation catch and release of these systems is currently ongoing.

Conflicts of interest

There are no conflicts to declare.

Acknowledgements

Notes and references

1   R. Klajn, J. F. Stoddart, and B. A. Grzybowski, *Chem. Soc. Rev.*, 2010, **39**, 2203.
2   M. Xue, Y. Yang, X. Chi, X. Yan, and F. Huang, *Chem. Rev.*, 2015, **115**, 7398.
3   (a) V. Blanco, D. A. Leigh, and V. Marco, *Chem. Soc. Rev.* 2015, **44**, 5341. (b) J. Choudhury, *Tetrahedron Lett.*, 2018, **59**, 487. (c) N. Kumagai, and M. Shibasaki, *Catal. Sci. Technol.*, 2013, **3**, 41.
4   G. Yu, K. Jie, F. Huang, *Chem. Rev.*, 2015, **115**, 7240. (b) P. Wei, X. Yan, F. Huang, *Chem. Soc. Rev.*, 2015, **44**, 815. (c) S. Dong, B. Zheng, F. Wang, F. Huang, *Acc. Chem. Res.*, 2014, **47**, 1982.
5   (a) S. Erbas-Cakmak, D. A. Leigh, C. T. McTernan, and A. L. Nussbaumer, *Chem. Rev.*, 2015, **115**, 10081–10206. (b) S. Kassem, T. van Leeuwen, A. S. Lubbe, M. R. Wilson, B. L. Feringa, and D. A. Leigh, *Chem. Soc. Rev.*, 2017, **46**, 2592–2621. (c) M. Baroncini, L. Casimiro, C. de Vet, J. Groppi, S. Silvi, and A. Credi, *ChemistryOpen*, 2018, **7**, 169–179.
6   Cucurbiturils and Related Macrocycles, K. Kim ed., Royal Society of Chemistry, Cambridge, 2020.
7   For selected reviews, see: (a) J. W. Lee, S. Samal, N. Selvapalam, H.-J. Kim, and K. Kim, *Acc. Chem. Res.*, 2003, **36**, 621. (b) K. Kim, N. Selvapalam, Y. H. Ko, K. M. Park, D. Kim, and J. Kim, *Chem. Soc. Rev.* 2007, **36**, 267. (c) S. J. Barrow, S. Kasera, M. J. Rowland, J. del Barrio, and O. A. Scherman, *Chem. Rev.*, 2015, **115**, 12320. (d) K. I. Assaf, and W. M. Nau, *Chem. Soc. Rev.*, 2015, **44**, 394.
8   (a) L. *Zhu*, M. Zhu, Y. Zhao, *ChemPlusChem*, 2017, **82**, 30. (b) E. Pazos, P. Novo, C. Peinador, A. E. Kaifer, and M. D. García, *Angew. Chem. Int. Ed.*, 2019, **58**, 403.
9   (a) P. M. S. Monk, *The Viologens: Physicochemical Properties, Synthesis, and Applications of the Salts of 4,4'-bipyridine*, John Wiley & Sons, Chichester, 1998; (b) P. M. S. Monk, R. D. Fairweather, J. A. Duffy and M. D. Ingram, *J. Chem. Soc., Perkin Trans. 2*, 1992, 2039.
10 For selected recent reviews on viologens: (a) M. Deska, J. *Kozlowska*, and W. Sliwa, *ARKIVOC*, 2013, **1**, 66. (b) L. Striepe, T. Baumgartner, *Chem. Eur. J.*, 2017, **23**, 16924. (c) K. Madasamy, D. Velayutham, V. Suryanarayanan, M. Kathiresan, and K.-C. Ho, *J. Mat. Chem. C*, 2019, **7**, 4622.
11 (a) A. Blanco-Gómez, I. Neira, J. L. Barriada, M. Melle-Franco, C. Peinador, and M. D. García, *Chem. Sci.*, 2019, **10**, 10680. (b) A. Blanco-Gómez, Á. Fernández-Blanco, V. Blanco, J. Rodríguez, C. Peinador, and Marcos D. Garcia, *J. Am. Chem. Soc.*, 2019, **141**, 3959. (c) I. Neira, C. Alvariño, O. Domarco, V. Blanco, C. Peinador, M. D. García, and J. M. Quintela, *Chem. Eur. J.*, 2019, **25**, 14834. (d) T. Rama, A. Blanco-Gómez, I. Neira, O. Domarco, M. D. García, J. M. Quintela, and C. Peinador, *Chem. Eur. J.*, 2017, **23**, 16743. (e) A. Blanco-Gómez, T. Rama, O. Domarco, I. Neira, V. Blanco,

J. M.; Quintela, M. D. García, and C. Peinador, *Dalton Trans.*, 2017, **46**, 1567. (f) O. Domarco, I. Neira, T. Rama, A. Blanco-Gómez, M. D. García, C. Peinador, J. M. Quintela, *Org. Biomol. Chem.*, 2017, **15**,3594. (g) T. Rama, E. M. López-Vidal, M. D. García, C. Peinador, J. M. Quintela, *Chem. Eur. J.*, 2015, **21**, 9482.

12   (a) I. Neira, A. Blanco-Gómez, J. M. Quintela, C. Peinador, and Marcos D. Garcia, *Org. Lett.*, 2019, **21**, 8976. (b) I. Neira, M. D. García, C. Peinador, and A. E. Kaifer, *J. Org. Chem.*, 2019, **84**, 2325.

13   K. Kim, D. Kim, J. W. Lee, Y. H. Ko and K. Kim, *Chem. Commun*., **2004**, 848.

14   (a) J. W. Lee, I. Hwang, W. S. Jeon, Y. H. Ko, S. Sakamoto, K. Yamaguchi, and K. Kim, *Chem. Asian J.*, 2008, **3**, 1277. (b) A. Trabolsi, M. Hmadeh, N. M. Khashab, D. C. Friedman, M. E. Belowich, N. Humbert, M. Elhabiri, H. A. Khatib, A.-M. Albrecht-Gary, and J. F. Stoddart, *New J. Chem.* 2009, **33**, 254.

15   A. E. Kaifer, W. Li, S. Silvi and V. Sindelar, *Chem. Commun*., 2012, **48**, 6693.

16   (a)T. M. Bockman, and J. K. Kochi*, J. Org. Chem.* 1990, **55**, 4127. (b) G. Ragazzon, C. Schäfer, P. Franchi, S. Silvi, B. Colasson, M. Lucarini, and A. Credi, *PNAS* 2018, **115**, 9385.

17   M. Marchini, M. Baroncini, G. Bergamini, P. Ceroni, M. D'Angelantonio, P. Franchi, M. Lucarini, F. Negri, T. Szreder, and M. Venturi, *Chem. Eur. J.* 2017, **23**, 6380.

18   (a) M. R. Geraskina, A. T. Buck, and A. H. Winter, *J. Org. Chem.* 2014, **79**, 7723. (b) A. G. Evans, J. C. Evans, and M. W. Baker, *J. Am. Chem. Soc.* 1977, **99**, 5882. (c) A. G. Evans, J. C. Evans, and M. W. Baker, *J. Chem. Soc. Perkin Trans. 2* 1975, 1310. (d) A. G. Evans, J. C. Evans, and M. W. Baker, *J. Chem. Soc. Perkin Trans. 2* 1977, 1787. (e) K. Tsukahara, J. Kaneko, T. Miyaji, K. Abe, M. Matsuoka, T. Hara, T. Tanase, and S. Yano, *Bull. Chem. Soc. Jpn.* 1999, **72**, 139. (f) A. T. Buck, J. T. Paletta, S. A. Khindurangala, C. L. Beck, and A. H. Winter, *J. Am. Chem. Soc.* 2013, **135**, 10594.